Neuron
NeuroResource

Recombinant Probes for Visualizing Endogenous Synaptic Proteins in Living Neurons

Garrett G. Gross,[1,7] Jason A. Junge,[2,7] Rudy J. Mora,[2,7] Hyung-Bae Kwon,[3] C. Anders Olson,[4] Terry T. Takahashi,[1] Emily R. Liman,[2] Graham C.R. Ellis-Davies,[5] Aaron W. McGee,[6] Bernardo L. Sabatini,[3] Richard W. Roberts,[1,*] and Don B. Arnold[2,*]
[1]Department of Chemistry
[2]Department of Biology
University of Southern California, Los Angeles, CA 90089, USA
[3]Howard Hughes Medical Institute, Department of Neurobiology, Harvard Medical School, Boston, MA 02115, USA
[4]Department of Molecular and Medical Pharmacology, University of California, Los Angeles, Los Angeles, CA 90090; USA
[5]Department of Neuroscience, Mount Sinai School of Medicine, New York, NY 10029, USA
[6]Saban Research Institute, Childrens Hopsital Los Angeles, Los Angeles, CA 90027, USA
[7]These authors contributed equally to this work
*Correspondence: richrob@usc.edu (R.W.R.), darnold@usc.edu (D.B.A.)
http://dx.doi.org/10.1016/j.neuron.2013.04.017

SUMMARY

The ability to visualize endogenous proteins in living neurons provides a powerful means to interrogate neuronal structure and function. Here we generate recombinant antibody-like proteins, termed *F*ibronectin *in*trabodies *g*enerated with m*R*NA display (FingRs), that bind endogenous neuronal proteins PSD-95 and Gephyrin with high affinity and that, when fused to GFP, allow excitatory and inhibitory synapses to be visualized in living neurons. Design of the FingR incorporates a transcriptional regulation system that ties FingR expression to the level of the target and reduces background fluorescence. In dissociated neurons and brain slices, FingRs generated against PSD-95 and Gephyrin did not affect the expression patterns of their endogenous target proteins or the number or strength of synapses. Together, our data indicate that PSD-95 and Gephyrin FingRs can report the localization and amount of endogenous synaptic proteins in living neurons and thus may be used to study changes in synaptic strength in vivo.

INTRODUCTION

Immunocytochemistry, a technique invented almost 70 years ago, has made it possible to visualize the spatial distribution of specific molecules in cells and tissues (Coons et al., 1942). Despite its utility, however, a number of properties of immunocytochemistry drastically limit the range of experimental questions to which it can be applied. For instance, staining of cytoplasmic proteins requires that cells first be fixed and permeabilized, which precludes its use in labeling live cells. Also, application of antibodies to tissue results in the labeling of all molecules within the tissue. Thus, it is often difficult to extract information about the localization of the molecule within an individual cell. Some of these limitations were overcome with the cloning of the gene encoding the green fluorescent protein (GFP) (Chalfie et al., 1994). GFP can be genetically fused to a protein of interest, making it possible to visualize that protein within living cells (Marshall et al., 1995). If GFP-tagged proteins are introduced into sparsely distributed cells, the subcellular localization of the protein can be easily interpreted, even in complex tissue preparations such as brain slices (Arnold and Clapham, 1999). However, introduced GFP-fusion proteins may fail to localize properly, due to saturation of targeting machinery, and overexpression of proteins can have dramatic morphological and/or functional effects on cells (El-Husseini et al., 2000). For instance, when the potassium channel Kv4.2 is exogenously expressed in neurons in culture or slices, it localizes diffusely to the somatodendritic region (Chu et al., 2006; Rivera et al., 2003), whereas endogenous Kv4.2 localizes in a conspicuously punctate manner (Burkhalter et al., 2006; Jinno et al., 2005). These problems may be circumvented by introducing tagged proteins into a knockout background (Lu et al., 2010) or by knocking GFP into the locus of the endogenous gene (Chiu et al., 2002). However, the former method may fail if the expression of the introduced transgene is not regulated at precisely the same level and with the same temporal pattern as the endogenous protein and the latter method is time consuming and costly. Moreover, both methods have three serious limitations that restrict their applicability: (1) they do not readily allow labeling of two or more proteins in the same cell, (2) it is difficult to confine the expression of the tagged proteins to a genetically defined subset of cells, and (3) they do not allow any analysis of either posttranslational modifications or specific protein conformations.

Recently, a novel strategy was used to label endogenous proteins in a manner that avoids the drawbacks associated with traditional approaches (Nizak et al., 2003). Recombinant antibody-like proteins (termed intrabodies) that bind to endogenous target proteins were selected from a library of single-chain antibodies, scFvs (Huston et al., 1988), using phage display. The genes encoding intrabodies were then fused to GFP genes and

transfected into cells in culture allowing an activated form of Rab6 to be visualized in real time. Phage display selection of scFv libraries has also been used to generate intrabodies against neuronal proteins such as Gephyrin and Huntingtin (Southwell et al., 2008; Varley et al., 2011). Nonetheless, this method has a serious drawback: the scFv scaffold requires disulfide bonds for stable folding, but the reducing environment of the cell precludes the formation of disulfide bonds. Thus, the scFv scaffold is prone to misfolding and/or aggregation (Goto and Hamaguchi, 1979; Goto et al., 1987; Proba et al., 1998). This problem was subsequently solved by using the 10^{th} fibronectin type III domain from human fibronectin (10FnIII) as a scaffold (Koide et al., 1998). This domain has an overall beta-sandwich topology and loop structure similar to the VH domain of IgG but folds stably with no disulfide bonds (Dickinson et al., 1994; Koide et al., 1998; Main et al., 1992). Libraries composed of 10FnIII domains have been combined with phage display selection to create binders to targets, such as one against the Src SH3 domain (Karatan et al., 2004), that work in reducing environments. Another innovation has been the use of mRNA display, an entirely in vitro selection method that uses libraries with $> 10^{12}$ sequences, 10^3- to 10^4-times higher diversity than phage display. This method has been used to create protein aptamers that bind to targets such as the SARS virus N-protein and phospho-iKappa-Balpha with very high target binding affinity and selectivity (Ishikawa et al., 2009; Olson et al., 2008; Olson and Roberts, 2007; Xu et al., 2002).

Despite these advances, intrabodies have not been widely used for imaging protein localization and expression. A central problem in the application of intrabodies to cellular imaging is that they are only expected to colocalize with the target protein if the expression level of the intrabody is the same as or lower than that of the cognate protein; otherwise, the unbound intrabody that is freely diffusible in the cytoplasm will overwhelm the image. Here we describe a method that overcomes these obstacles and allows endogenous protein to be visualized in real time in living cells. Our method is based on the generation of disulfide-free intrabodies, known as FingRs, that are transcriptionally regulated by the target protein. Specifically, we used a 10FnIII-based library in combination with mRNA display to identify FingRs that bind two synaptic proteins, Gephyrin and PSD95. After the initial selection, we screened binders using a cellular localization assay to identify potential FingRs that bind at high affinity in an intracellular environment. We also created a transcriptional control system that matches the expression of the intrabody to that of the target protein regardless of the target's expression level. This system virtually eliminates unbound FingR, resulting in very low background that allows unobstructed visualization of the target proteins. Thus, the FingRs presented in this study allow excitatory and inhibitory synapses to be visualized in living neurons in real time, with high fidelity, and without affecting neuronal function.

RESULTS

Generating FingRs that bind to PSD-95 or Gephyrin

Our goal in this work was to create reagents that could be used to label excitatory and inhibitory synapses in live neurons. To do this, we chose two well-established protein targets that serve as immunocytochemical markers for these structures: PSD-95, a marker of excitatory postsynaptic sites (Cho et al., 1992), and Gephyrin, a marker of inhibitory postsynaptic regions (Craig et al., 1996; Langosch et al., 1992; Prior et al., 1992; Takagi et al., 1992). Within each protein, we targeted well-structured regions where binding to FingRs would be unlikely to disturb function. For PSD-95 we chose the SH3-GK domain, which mediates intra- and intermolecular interactions (McGee et al., 2001), while for Gephyrin, we chose the G domain, which mediates trimerization (Sola et al., 2001). In the case of Gephyrin we used protein in a trimerized state as a target in order to generate binders to the external surface.

To isolate FingRs, we generated recombinant disulfide-free antibody-like proteins based on the Fibronectin 10FnIII scaffold using mRNA display (Roberts and Szostak, 1997). The naive FingR library was constructed as described (Olson and Roberts, 2007), with the addition of point mutations that enhance expression and folding (Olson et al., 2008). The resulting library was predominantly full-length, in-frame clones and had an expressed diversity of $> 10^{12}$ proteins spread over 17 residues in the BC and FG loops (Figure 1A).

Using this library, two selections were performed—one targeting Gephyrin and one targeting PSD-95 (Figure 1B). In each case, the target protein was immobilized on a solid support and used to purify functional library members via affinity chromatography. The purified mRNA-protein fusions were then amplified to provide a new library enriched for binders to the targets, which was used for the next round of selection. After six rounds, the number of PCR cycles needed to generate the enriched pool decreased markedly, indicating that both selections had converged to predominantly functional clones. A radioactive pull-down assay confirmed this observation (Figures 1C and 1D), demonstrating that 42% of the Gephyrin FingR pool (round 7) and 45% of the PSD-95 FingR pool (round 6) bound to target with very low background binding. Importantly, cloning and sequencing of each pool indicated that both contained numerous, independent, functional FingRs.

Since numerous independent FingRs bound to target, we wished to choose proteins that gave the best intracellular labeling. To do this, we devised a stringent COS cell screen, wherein the target (e.g., Gephyrin) was localized to the cytoplasmic face of the Golgi apparatus by appending a short Golgi-targeting sequence (GTS) (Andersson et al., 1997) (Figure 1E). Functional FingRs ("winners") were defined as those that showed tight subcellular colocalization between the rhodamine-labeled target and the GFP-labeled FingR (Figures 1F–1H). Suboptimal sequences (Figure 1I, "losers") result in diffuse staining (Figure 1K), poor expression, and/or poor colocalization (Figures 1J and 1L). This experiment allowed us to choose FingR proteins that satisfied three essential criteria: (1) good expression and folding inside a mammalian cell, (2) lack of aggregation, and (3) high-affinity binding to the intended target under cellular conditions and despite the high levels of other proteins present. Our results confirm the importance and stringency of the screen, as only 10%–20% of FingR clones (4/30 PSD-95 FingRs and 3/14 Gephyrin FingRs) that bind to the target in vitro colocalized with target intracellularly.

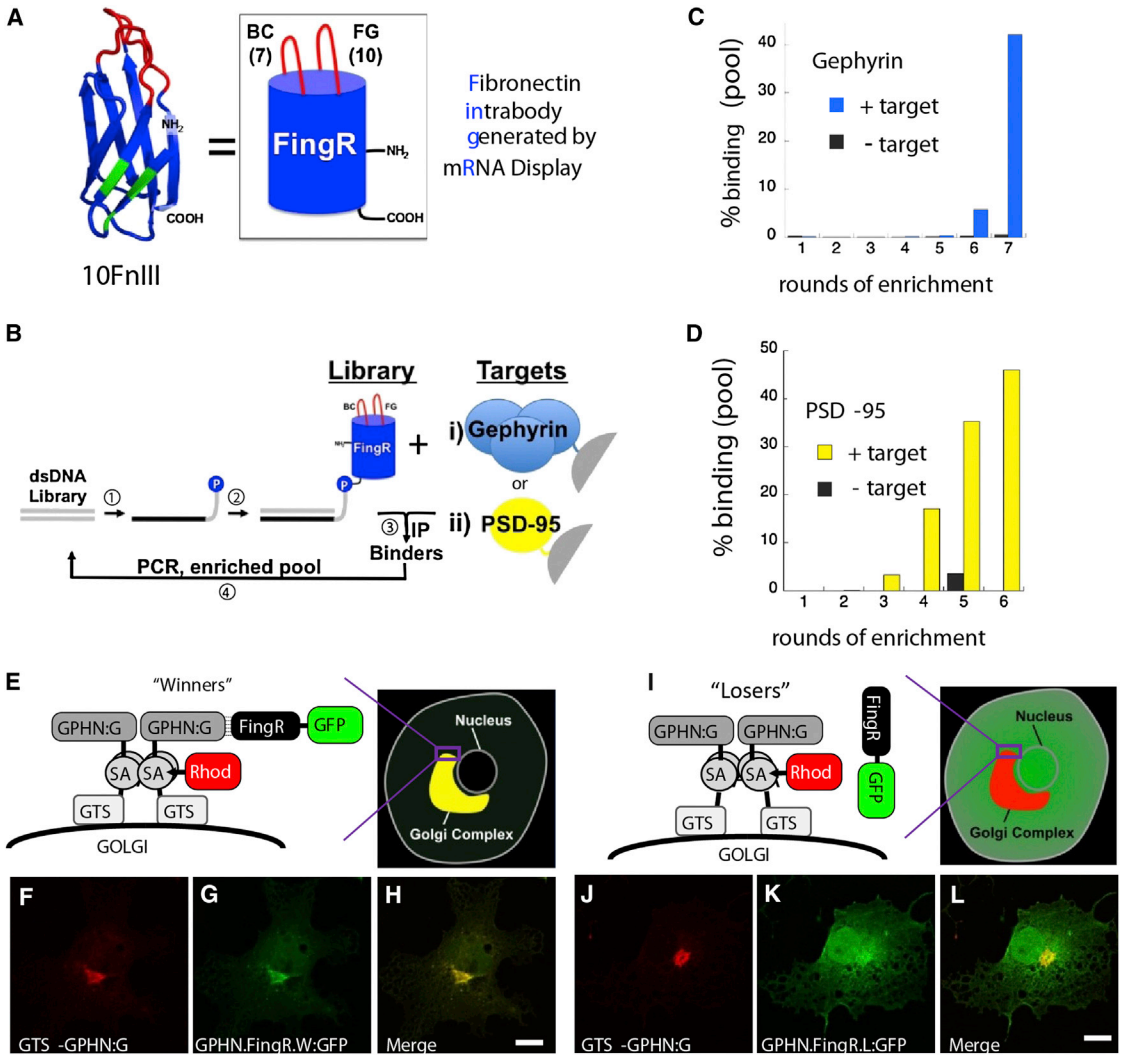

Figure 1. Selection of Fibronectin Binders of PSD-95 and Gephyrin by mRNA Display and by a Cellular Localization Assay

(A) A library consisting of 10FnIII domains with 17 random residues in the BC and FG loops was used to select binders to PSD-95 and Gephyrin.

(B) The selection protocol is as follows: (1) DNA encoding the randomized Fibronectins was transcribed and a puromycin molecule attached to linker DNA was fused to the 3′ end of the transcript. (2) The mRNA-puromycin fusion was translated to give an mRNA-puromycin-peptide molecule. An anti-sense cDNA strand hybridized to the mRNA was synthesized that allows individual library members to be amplified by PCR. (3) The library was exposed to target molecules consisting of either the G domain of Gephyrin or the SH3-GK domains of PSD-95. Binders were purified by precipitation. (4) Library members that bound were amplified by PCR to reconstitute a library that is enriched for binders to target.

(C and D) Percentage of the library that bound to the beads after each round of selection.

(E) Schematic of a COS cell expressing (1) a FingR that binds to its target with high affinity (winner) and (2) the target domain from the selection (GPHN:G) fused to a Golgi targeting sequence (GTS) and Streptavidin (SA) and tagged with biotin-Rhodamine (Rhod). If the FingR-GFP binds to the target domain with high affinity and specificity, it becomes localized to the Golgi apparatus and colocalized with GTS-GPHN:G.

(F and G) Expression pattern of GTS-GPHN:G tagged with Rhodamine (red, F) colocalizes with that of GPHN.FingR.W-GFP (green, G).

(H) Yellow indicates colocalization of GTS-GPHN:G and GPHN.FingR.W-GFP.

(I) Schematic of COS cell expressing GTS-GPHN:G and a FingR that does not bind to target with high affinity and specificity, GPHN.FingR.L-GFP.

(J and K) Expression pattern of GTS-GPHN:G tagged with Rhodamine (red, J) does not colocalize with that of GPHN.FingR.L-GFP, but instead localizes diffusely (green, K).

(L) A relative lack of yellow staining in merge of GTS-GPHN:G and GPHN.FingR.L-GFP indicates a lack of colocalization. Scale bar represents 5 μm.

PSD95 and Gephyrin FingRs Label Endogenous Targets in Neurons in Culture

For determining whether FingRs can label endogenous Gephyrin or PSD-95 in native cells, GFP-tagged FingR cDNAs that were positive in the COS cell assay were expressed in dissociated cortical neurons in culture. After incubation for 14 hr, the cultures were fixed and immunostained for both GFP and the endogenous target proteins. In each selection,

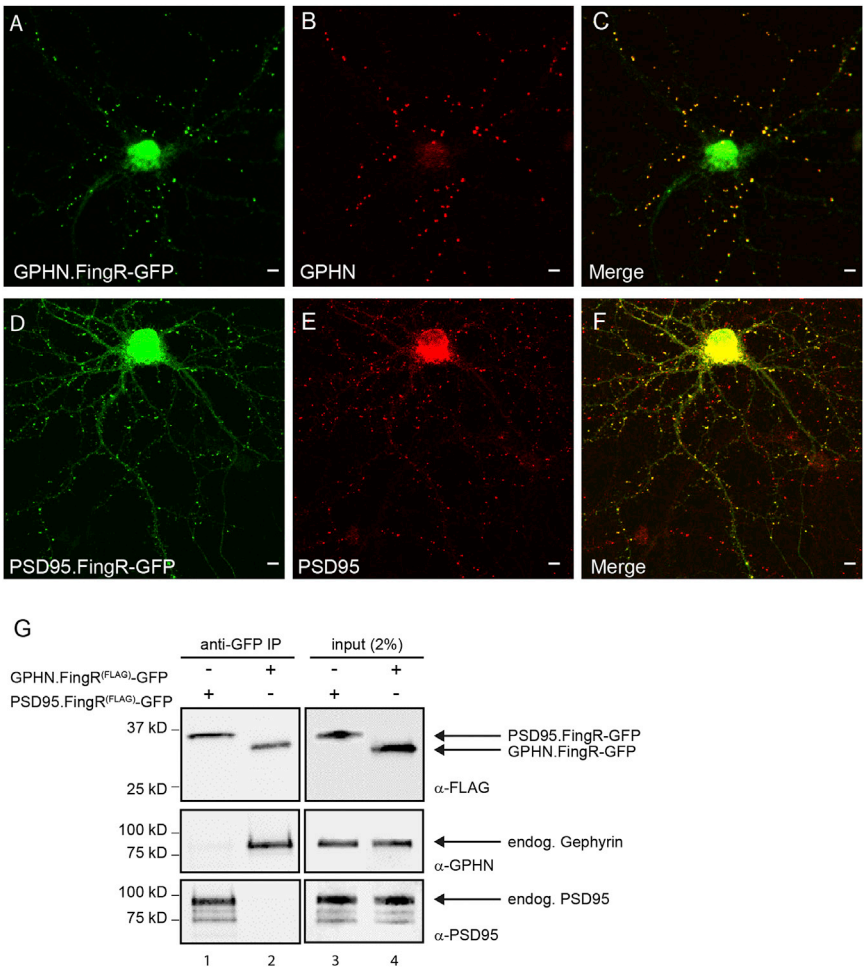

Figure 2. FingRs Recognizing Gephyrin or PSD-95 Bind to Endogenous Targets after Expression in Neurons

(A) A FingR against Gephyrin (GPHN.FingR-GFP, green) localizes in a punctate fashion after expression in a dissociated cortical neuron.

(B) Endogenous Gephyrin (red).

(C) Merge of GPHN.FingR-GFP and endogenous Gephyrin shows colocalization (yellow).

(D) A FingR against PSD-95 (PSD95.FingR-GFP, green) localizes in a punctate fashion after expression in a cortical neuron.

(E) Endogenous PSD-95 (red).

(F) Merge of PSD95.FingR-GFP and endogenous PSD-95 shows colocalization (yellow). Scale bar represents 5 μm.

(G) Coimmunoprecipitation of endogenous target proteins with FingRs after expression in cortical neurons in culture. Neurons were infected with lentivirus expressing either PSD95.FingR$^{(FLAG)}$-GFP (lanes 1, 3) or GPHN.FingR$^{(FLAG)}$-GFP (lanes 2, 4), both of which contained a FLAG-tag that enabled immunolabeling. After 96 hr of expression, cells were lysed and a portion of the lysates were exposed to a bead-linked anti-GFP antibody. The resulting precipitates were run on an SDS PAGE gel (lanes 1, 2) along with the lysates (lanes 3, 4), blotted, and probed with anti-FLAG antibodies (top), anti-Gephyrin antibodies (middle), and anti-PSD-95 antibodies (bottom). PSD95.FingR$^{(FLAG)}$-GFP coimmunoprecipitated with endogenous PSD95, but not with endogenous Gephyrin, whereas GPHN.FingR$^{(FLAG)}$-GFP coimmunoprecipitated with Gephyrin, but not with PSD95.

See also Figure S1.

at least one FingR (PSD95.FingR for PSD-95, GPHN.FingR for Gephyrin) localized in a punctate manner characteristic of both target proteins (Figures 2A and 2D). The expression patterns of each FingR showed striking colocalization with its cognate endogenous protein (Figures 2B, 2C, 2E, and 2F). In addition, when GPHN.FingR-GFP was expressed in either excitatory or inhibitory neurons it appeared in puncta adjacent to or overlapping presynaptic terminals labeled for GAD-65 (Figure S1 available online). These results are consistent with FingRs binding at high affinity to PSD-95 or Gephyrin. To corroborate the results from colocalization experiments we used biochemical means to test for interaction between each FingR and its endogenous target protein in cortical neurons in culture. cDNAs encoding each FingR were incorporated into a lentivirus, which was used to infect the cultures. After expression of either PSD95.FingR-GFP or GPHN.FingR-GFP for 96 hr, we collected cell lysate, which was exposed to immobilized anti-GFP antibody. The immunoprecipitated protein complexes were blotted and stained for the presence of the endogenous target proteins. In cells infected with PSD95.FingR-GFP, the anti-GFP antibody coimmunoprecipitated a band at 95 kD that was labeled by the anti-PSD-95 antibody (Figure 2G), but the precipitate was not labeled with anti-Gephyrin antibodies. In cells where GPHN.FingR-GFP was expressed, the precipitate pulled down by the anti-GFP antibody contained a band at 80 kD that was labeled with the anti-Gephyrin antibody, but the precipitate was not labeled with the anti-PSD-95 antibody (Figure 2G).

The GK domain of PSD95, which is contained within the target of the PSD95.FingR selection, interacts with guanylate kinase-associated protein (GKAP), a protein that links PSD-95 to Shank-Homer complexes (Naisbitt et al., 1999; Tu et al., 1999) and has been implicated in synaptic remodeling (Shin et al., 2012). To determine whether binding of PSD95.FingR with PSD-95 interferes with the interaction between PSD-95 and GKAP, we asked whether GKAP could pull down both PSD-95 and PSD95.FingR-GFP when all three proteins were expressed in COS cells. We found that, indeed, immunoprecipitation of GKAP resulted in coprecipitation of both PSD-95 and PSD95.FingR-GFP (Figure S1). Furthermore, in COS cells expressing only GKAP and PSD95.FingR-GFP, immunoprecipitation of GKAP did not cause coprecipitation of PSD95.FingR-GFP. Thus, in the GKAP/PSD95/PSD95.FingR-GFP complex, GKAP and PSD95.FingR must both bind to PSD95, indicating that binding of PSD95.FingR to PSD-95 does not disrupt binding of PSD-95 to GKAP.

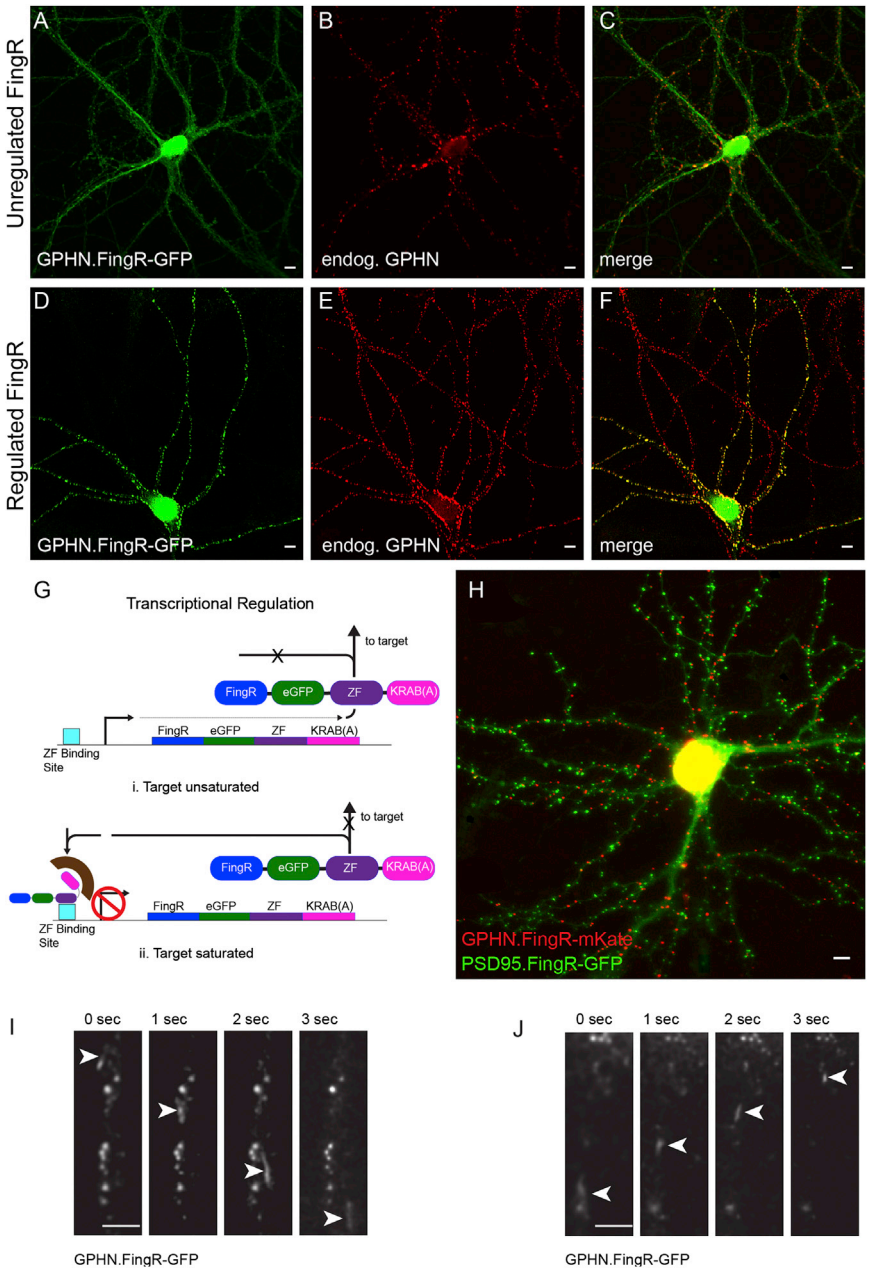

Figure 3. A Transcriptional Control System Causes FingRs to Be Expressed at the Same Level as the Endogenous Target Protein

(A) GPHN.FingR-GFP (green) expressed for 7 days localizes in a nonspecific pattern, probably due to high background from unbound FingR.

(B and C) Endogenous Gephyrin (red) does not colocalize with GPHN.FingR-GFP.

(D–F) GPHN.FingR-GFP (green, D) with transcriptional regulation expressed for 7 days appears in a punctate pattern that precisely colocalizes with that of endogenous Gephyrin (red, E; yellow, F). Note that red staining that does not colocalize in (F) is from untransfected cells. Scale bar represents 5 μm.

(G) To control its transcription the FingR (blue) is fused to a transcription factor consisting of a zinc finger DNA binding domain (ZF, purple) fused with a KRAB(A) transcriptional repressor domain (pink). In addition, a ZF DNA binding site (light blue) was inserted upstream of the CMV promoter. When less than 100% of the target is bound by FingR (i), then 100% of newly made FingR binds to endogenous target and is prevented from moving to the nucleus. When 100% of the target is bound (ii), then newly made FingR can no longer bind to the target and, instead, moves to the nucleus as a result of the nuclear localization signal within the ZF. Once in the nucleus the transcription factor binds to the ZF binding site and represses transcription. Thus, the level of FingR is matched to the level of the endogenous target protein.

(H) Live cortical neuron coexpressing regulated PSD95.FingR-GFP (green) and GPHN.FingR-mKate2 (red). Note that the regulation systems for PSD95.FingR-GFP and GPHN.FingR-mKate2 are based on DNA binding domains from CCR5 and IL2RG, respectively. Each FingR is expressed in a punctate, nonoverlapping fashion consistent with labeling of PSD-95 and Gephyrin.

(I) Neuron in cortical culture expressing transcriptionally controlled GPHN.FingR-GFP after lentiviral infection. Images taken at 1 s intervals show a vesicle moving with a velocity of ~7 $\mu m.s^{-1}$ in the axon.

(J) Similarly labeled vesicle moving at ~4 $\mu m.s^{-1}$ in the axon. Scale bar represents 5 μm.

See also Figure S2 and Movie S1.

A Transcriptional Control System to Regulate the Expression Level of FingRs

In order for FingRs to accurately report the localization and trafficking of their endogenous targets, it is necessary to minimize the excess, unbound FingR. To demonstrate the effect of overexpressing FingRs, we expressed either GPHN.FingR-GFP (Figures 3A–3C) or PSD95.FingR-GFP (Figure S2) for periods of 48 hr to 6 days and found that each appears in a diffuse pattern consistent with the signal from the excess, unbound FingR overwhelming the signal from the FingR bound to its target (Figures 3A–3C, Figure S2). In order to minimize this background signal, we developed a transcriptional control system that was designed to closely match the expression level of a FingR with that of its endogenous target (Figure 3G). This transcriptional control system uses the transcription repressor KRAB(A) fused to a ZINC-finger (ZF) binding domain (Margolin et al., 1994; Witzgall et al., 1994). In our system ZF fused to KRAB(A) is fused to the FingR itself and ZF binding sites are inserted into the DNA upstream of the promoter that controls FingR expression (Figure 3G). When bound to target proteins in the dendrites, via FingRs, ZF-KRAB(A) is physically prevented from moving to the nucleus and turning off transcription (Figure 3G). Thus, as long as there is unbound target present the ZF-KRAB(A) transcription factor will be prevented from turning off transcription.

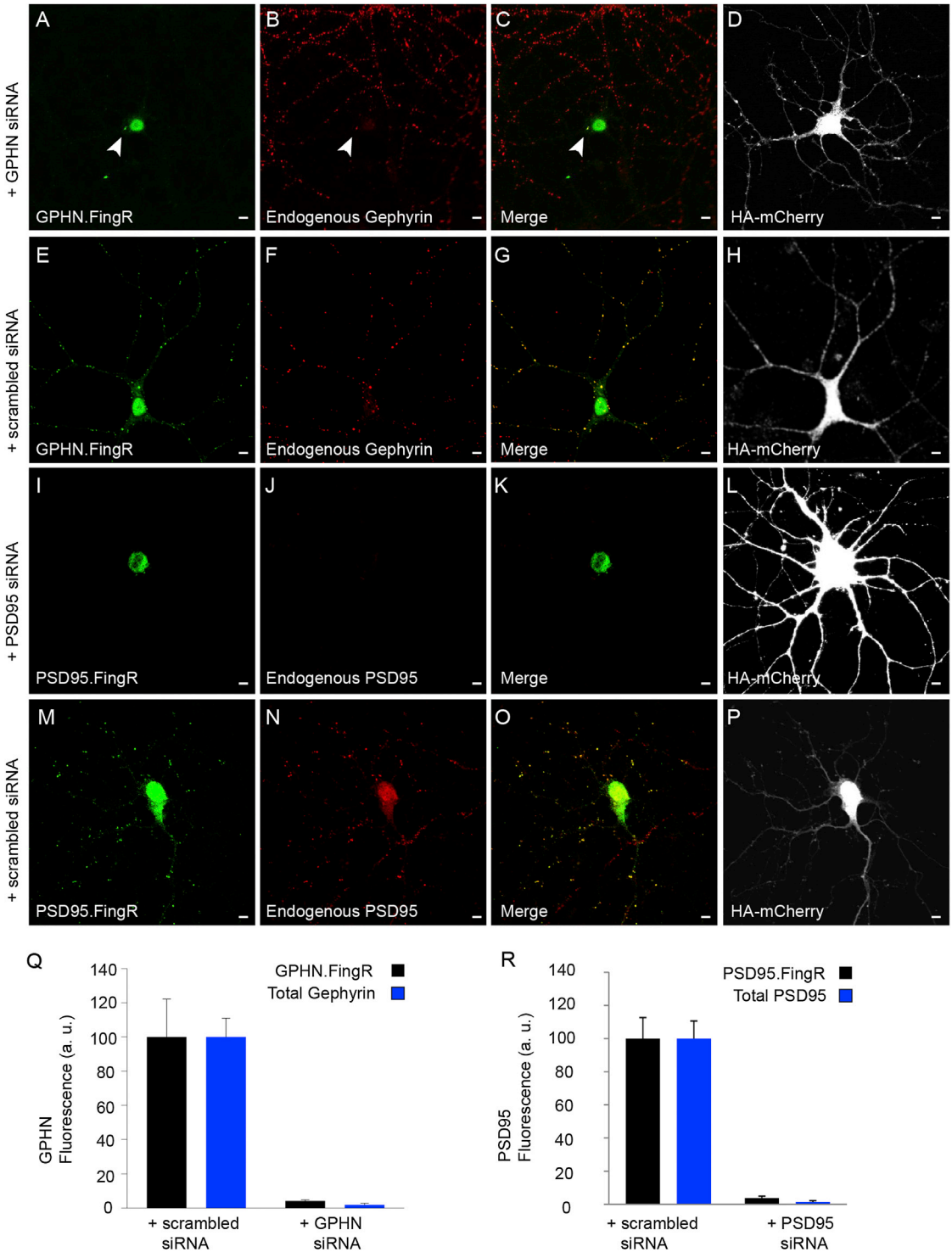

Figure 4. Knockdown of Gephyrin or PSD-95 in Dissociated Cortical Neurons Leads to Elimination of GPHN.FingR and PSD95.FingR Staining

(A–D) Cortical neuron in dissociated culture coexpressing siRNA against Gephyrin and the transcriptionally controlled GPHN.FingR (A). Note that virtually no staining against the GPHN.FingR is visible in the dendrites or axon except for a single punctum (arrowhead), which colocalizes with a punctum of endogenous Gephyrin (B and C).

HA-mCherry staining of the transfected cell (D). (E–H) In contrast, when the transcriptionally regulated GPHN.FingR was coexpressed with scrambled siRNA it expressed abundantly in a punctate pattern (E) that colocalized with endogenous Gephyrin (F and G).

(H) HA-mCherry staining of the transfected cell.

(legend continued on next page)

However, if all of the target is bound, the unbound ZF-KRAB(A) transcription factor moves to the nucleus and turns off transcription. In this manner the expression level of the FingR should be closely matched to that of its target.

To test whether this transcriptional control system can effectively regulate the expression level of FingRs, we expressed transcriptionally controlled versions of GPHN.FingR-GFP or PSD95.FingR-GFP in cortical neurons in culture for 7 days. Both transcriptionally controlled FingRs localized in a punctate manner, precisely colocalizing with their target proteins (Figures 3D–3F; Figure S2), in contrast to the nonspecific localization of the uncontrolled FingRs (Figures 3A–3C; Figure S2). To quantitate the degree to which transcriptionally controlled and uncontrolled FingRs localized to postsynaptic sites, we calculated the ratio of the amount of FingR at nonsynaptic sites on dendrites versus at postsynaptic sites ($R_{n/s}$). $R_{n/s}$ for uncontrolled GPHN.FingR-GFP was 0.96 ± 0.16 (n = 100 synapses) as compared with 0.033 ± 0.005 (n = 100) for the same construct with transcriptional control and 0.002 ± 0.006 for endogenous Gephyrin (Figure S2). Similarly, $R_{n/s}$ for unregulated PSD95.FingR-GFP was 0.90 ± 0.02, 0.16 ± 0.01 for regulated PSD95.FingR-GFP, and 0.16 ± 0.008 for endogenous PSD-95 (Figure S2). Thus, our results are consistent with the transcriptional control drastically reducing the amount of unbound FingR that contributes to background signal. Note that the transcriptional control system causes the accumulation of some FingR in the nucleus (Figure S2).

To further test the transcriptional control system, we asked whether regulated FingRs could maintain high-fidelity labeling in response to a sudden increase in target protein. To simulate such an increase, we first transfected cortical neurons in culture with an inducible construct containing Gephyrin-mKate2 along with a second construct containing transcriptionally regulated GPHN.FingR-GFP, but without inducing transcription of Gephyrin-mKate2. After 1 week in culture, expression of Gephyrin-mKate2 was induced by adding an Ecdysone analog for 24 hr. This induction of Gephyrin-mKate2 produced an increase in total Gephyrin staining of approximately 110% versus uninduced cells as measured by immunocytochemistry (Figure S2). A similar increase was seen in GPHN.FingR-GFP staining between induced versus uninduced, consistent with a coordinated upregulation of FingR expression. To quantify the relative fidelity with which GPHN.FingR-GFP-labeled uninduced versus induced cells, we calculated the ratio of total Gephyrin staining versus GPHN.FingR-GFP staining at individual puncta. We found that the ratio of total Gephyrin staining versus GPHN.FingR-GFP staining was 1.40 ± 0.03 (n = 200 puncta, 10 cells) for uninduced versus 1.47 ± 0.06 (n = 200 puncta, 10 cells) for induced cells. The two ratios are not significantly different (p = 0.15, Wilcoxon), indicating that GPHN.FingR-GFP labeled Gephyrin with similar fidelity in the uninduced versus induced cells, a result that is consistent with the transcriptional regulation system responding to the increase in target with an appropriately graded increase in FingR production.

To test whether the transcriptional regulation system could work for two FingRs simultaneously, we coexpressed PSD95.FingR-GFP and GPHN.FingR-mKate2 for 7 days. Both had independently regulated transcriptional control systems. PSD95.FingR-GFP was fused to the CCR5L zinc finger (Mani et al., 2005), and GPHN.FingR-mKate2was fused to the $IL2RG_2L$ zinc finger (Gabriel et al., 2011). PSD95.FingR-GFP and GPHN.FingR-mKate2 each expressed in a distinctly punctate manner with very little background or overlap between the two (Figure 3H), indicating that each transcriptional feedback system worked efficiently and independently.

To this point our experiments have concentrated on using FingRs to visualize the localization of endogenous proteins at single points in time. However, because FingRs can be visualized in living cells, it should be possible to use them to observe trafficking of their endogenous target proteins. To visualize trafficking of Gephyrin we used lentivirus to express transcriptionally controlled GPHN.FingR-GFP in neurons in culture for 7 days. Time-lapse imaging of these cultures revealed numerous vesicles moving in both directions in the cell body, axons, and dendrites (Figures 3I and 3J). Interestingly, axonal vesicles appeared more elongated and moved at higher velocity than dendritic vesicles, hitting speeds of $\sim$7 $\mu m.s^{-1}$ (Movie S1). Thus, GPHN.FingR-GFP can be used to visualize trafficking of endogenous Gephyrin in addition to its localization.

Testing FingRs for Binding Specificity and Off-Target Effects

To test whether FingRs label their endogenous targets specifically in cortical neurons in culture, we expressed either transcriptionally controlled PSD95.FingR-GFP or GPHN.FingR-GFP along with siRNA against either PSD-95 or Gephyrin. Cells in which either endogenous PSD-95 or endogenous Gephyrin was knocked down expressed extremely low levels of the corresponding FingR (Figures 4A–4D, 4I–4L, and S3). In contrast, cells expressing either PSD95.FingR or GPHN.FingR along with scrambled siRNA expressed considerably higher levels of each FingR. In addition, each FingR was expressed in a punctate

(I–L) Neuron expressing transcriptionally controlled PSD95.FingR and siRNA (I) shows a very low level of FingR staining that is comparable to the level of endogenous PSD-95 staining (J and K).

HA-mCherry staining of transfected cell (L). M-P In contrast, staining of the transcriptionally regulated PSD95.FingR is robust in a cell coexpressing scrambled siRNA (M) and colocalizes with staining of endogenous PSD-95.

(P) HA-mCherry staining of transfected cell. Scale bar represents 5 μm.

(Q) Quantitative comparison of the total amount of staining by anti-Gephyrin antibody (total Gephyrin) and by GPHN.FingR-GFP in the processes of neurons transfected with siRNA against Gephyrin versus with scrambled siRNA. Note that staining by anti-Gephyrin antibody and by GPHN.FingR-GFP are reduced by comparable amounts in cells expressing Gephyrin siRNA versus scrambled siRNA.

(R) Quantitative comparison of the total amount of staining by anti-PSD-95 antibody (total PSD95) and by PSD95.FingR-GFP in the processes of neurons transfected with siRNA against PSD-95 versus with scrambled siRNA. Note that staining by anti-PSD-95 antibody and by PSD95.FingR-GFP are reduced by comparable amounts in cells expressing PSD-95 siRNA versus scrambled siRNA.

All error bars represent SEM. See also Figure S3.

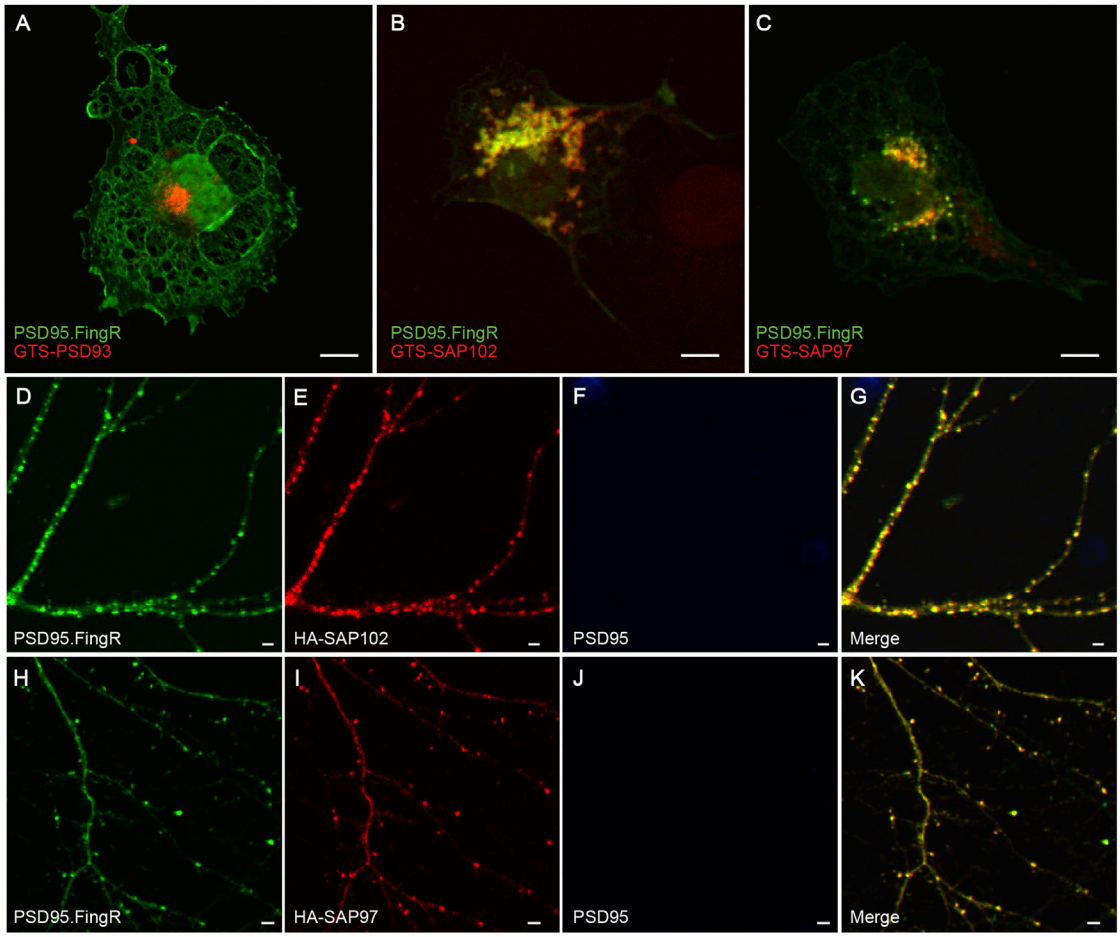

Figure 5. Interaction of PSD95.FingR with MAGUK Proteins

(A–C) In a COS cell coexpressing Golgi-targeted PSD-93 (GTS-PSD-93) and PSD95.FingR (A), the two proteins do not colocalize, indicating the PSD95.FingR does not interact with PSD-93. In contrast, PSD95.FingR colocalizes with GTS-SAP-102 (B) or GTS-SAP-97 (C) when it is coexpressed with either MAGUK protein.

(D–G) PSD95.FingR (D) colocalizes with exogenous HA-SAP-102 (E and G) after expression in dissociated cortical neurons where PSD-95 (F) has been knocked down with siRNA.

(H–K) PSD95.FingR (H) colocalizes with exogenous HA-SAP-97 (I and K) after expression in dissociated cortical neurons where PSD-95 (J) has been knocked down with siRNA. Scale bar represents 5 μm.

pattern that localized with the corresponding endogenous protein (Figures 4E–4H, 4M–4P, and S3). In the presence of siRNA against Gephyrin, the total Gephyrin expressed in processes per cell was reduced by 96% ± 1% (Figure 4Q; n = 10 cells) compared with scrambled siRNA, whereas the staining of GPHN.FingR-GFP was reduced by 98.1% ± 1% (n = 10 cells) under the same circumstances, a difference that is not significant ($p > 0.13$, t test). Similarly, in cells where the amount of total PSD-95 was reduced by 96% ± 1% (Figure 4R; n = 10 cells), the amount of PSD95.FingR staining in processes was reduced by 99% ± 1% (n = 10 cells) compared with cells expressing scrambled siRNA, a difference that is not significant ($p > 0.1$, t test). These results are consistent with the majority of PSD95.FingR and GPHN.FingR labeling their target proteins within dissociated cortical neurons.

In the CNS there are three close homologs of PSD-95 that are also found at postsynaptic sites: PSD-93, SAP-97, and SAP-102 (Brenman et al., 1998). To determine whether PSD95.FingR could distinguish between different MAGUK proteins, we independently tested whether PSD95.FingR-GFP bound to PSD-93, SAP-102, or SAP-97 in our COS cell assay. We found that PSD-93 did not colocalize with PSD95.FingR-GFP, whereas SAP-102 and SAP-97 did (Figures 5A–5C). To determine whether SAP-102 and SAP-97 interact with PSD95.FingR-GFP in a more stringent assay, we coexpressed HA-tagged versions of these proteins in cultured cortical neurons where PSD-95 expression had been knocked down with siRNA. We found that when PSD95.FingR is coexpressed with either SAP-97 or SAP-102, the coexpressed proteins colocalize (Figures 5D–5K). Thus, PSD95.FingR probably binds to heterologous SAP-97 and SAP-102 with relatively high affinity, but not to heterologous PSD-93. Additional testing will be required to determine the exact specificity of binding of PSD95.FingR-GFP with endogenous MAGUK proteins in vivo. However, even in the

case where PSD95.FingR does identify other synaptic MAGUK proteins, it is still suitable for marking synapses.

In addition to testing the specificity of binding, we asked whether expression of the FingR had a morphological effect on cells. In light of the dramatic increase in spine size and density caused by overexpression of PSD-95 (El-Husseini et al., 2000; Kanaani et al., 2002) and the large aggregates seen with overexpression of Gephyrin (Yu et al., 2007), we tested whether expression of PSD95.FingR-GFP or GPHN.FingR-GFP had an effect on the size of PSD-95 or Gephyrin puncta, respectively. We found that the amounts of total Gephyrin associated with individual puncta (stained with an anti-Gephyrin antibody) were nearly identically distributed in cells expressing GPHN.FingR-GFP (μ_{GPHN} = 18.1 ± 0.7 a.u., n = 200 puncta) versus with untransfected cells (μ_{GPHN} = 18.4 ± 0.8 a.u., n = 200, $p > 0.8$; Figures 6A, 6B, and S4). Similar results were also obtained for PSD-95 puncta in PSD95.FingR-GFP expressing cells ($\mu_{PSD\text{-}95}$ = 20 ± 2 a.u., n = 200) and in untransfected cells ($\mu_{PSD\text{-}95}$ = 20 ± 2 a.u., n = 200, $p > 0.5$; Figures 6E, 6F, and S4). In contrast, puncta from cells expressing Gephyrin-GFP contained significantly more total Gephyrin (μ_{GPHN} = 55 ± 3 a.u., n = 200) than puncta from comparable untransfected cells (μ_{GPHN} = 21 ± 1 a.u., n = 200, $p < 0.001$; Figures 6C, 6D, and S4). Similar measurements in cells expressing PSD95-GFP ($\mu_{PSD\text{-}95}$ = 41 ± 2 a.u., n = 200) were also higher than in untransfected cells ($\mu_{PSD\text{-}95}$ = 18 ± 1 a.u., n = 200, $p < 0.001$; Figures 6G, 6H, and S4). In addition, many cells expressing Gephyrin-GFP exhibited large aggregates of protein, as was observed previously (Yu et al., 2007). Such aggregates were never seen in cells expressing transcriptionally controlled GPHN.FingR-GFP. Thus, expressing GFP-tagged FingRs does not affect the size of Gephyrin or PSD-95 puncta, in contrast to overexpressed, tagged PSD-95 and Gephyrin.

PSD95.FingR and GPHN.FingR Do Not Affect the Electrophysiological Properties of Neurons

To further test PSD95.FingR and GPHN.FingR in a context that is closer to in vivo, we expressed them in organotypic rat hippocampal slices using biolistic transfection. Slices cut from rats at 8 days postnatal, transfected 2–3 days later, and then incubated for 7–8 days were imaged live using two-photon microscopy. Both transcriptionally controlled PSD95.FingR-GFP and GPHN.FingR-GFP expressed in a punctate pattern that was similar to their respective localization patterns after expression in dissociated neurons (Figures 7A and 7F). Furthermore, PSD95.FingR-GFP was clearly concentrated in dendritic spines, while GPHN.FingR-GFP was found in puncta on the dendritic shaft, consistent with the former being localized to postsynaptic excitatory sites and the latter being localized to postsynaptic inhibitory sites. The morphology of neurons transfected with PSD95.FingR-GFP was not different from untransfected cells, and, in particular, spine density did not differ significantly between cells expressing PSD95.FingR-GFP (Figure 7B; spine density = 0.94 ± 0.08 spines.μm^{-1}; n = 1,064 spines, 8 cells) and control cells, (spine density = 0.97 ± 0.06 spines.μm^{-1}; n = 1,396 spines, 9 cells; $p > 0.5$, t test). In order to determine whether expressing FingRs had a physiological effect on cells we measured spontaneous miniature excitatory postsynaptic currents (mEPSCs) in neurons expressing PSD95.FingR-GFP and spontaneous miniature inhibitory postsynaptic currents (mIPSCs) in neurons expressing GPHN.FingR-GFP. We found that neither mEPSCs nor mIPSCs from cells expressing the corresponding FingR differed qualitatively from untransfected control cells (Figures 7C and 7G). In addition, in cells expressing PSD95.FingR-GFP mEPSC frequency (f) and amplitude (A) measurements (f = 1.59 ± 0.1 s^{-1}, A = 9.7 ± 0.6 pA, n = 8 cells) did not differ significantly from that in control cells (Figures 7D and 7E; f = 1.66 ± 0.2 s^{-1}, A = 10.8 ± 0.7 pA, n = 8 cells; $p > 0.5$ t test). Similarly, measurements of frequencies and amplitudes of mIPSCs in cells expressing GPHN.FingR-GFP (Figures 7H and 7I; f = 4.2 ± 0.5 s^{-1}, A = 14.1 ± 1.0 pA, n = 8 cells) were not significantly different from comparable measurements in control cells (f = 4.3 ± 0.5 s^{-1}, A = 13.5 ± 1.1 pA, n = 9 cells; $p > 0.1$ t test). Thus, our results indicate that expressing PSD95.FingR-GFP and GPHN.FingR-GFP does not cause changes in synaptic physiology and has no effect on the number or neurotransmitter receptor content of individual synapses.

To determine whether GPHN.FingR-GFP signals represent functional inhibitory synapses, we measured IPSCs evoked by GABA photolysis at individual green punta. Hippocampal CA1 pyramidal neurons were transfected with GPHN.FingR-GFP and TdTomato to visualize inhibitory synapses and neuronal structure (Figure 8A). Two-photon GABA uncaging 0.5 μm away from puncta of GPHN.FingR-GFP triggered IPSCs. IPSC amplitude diminished when uncaging occurred further away from the dendrite, demonstrating that IPSCs originated from the activation of receptors localized in dendrites of the recorded neuron (Figures 8B and 8C). When GABA was photoreleased on the dendritic shaft at locations where GPHN.FingR-GFP was present, robust IPSCs were evoked. However, GABA photorelease at two locations, one in a dendritic spine and a second on a dendritic shaft, where there was no GPHN.FingR-GFP signal elicited small or negligible IPSCs (Figures 8D and 8E). These data confirm that GPHN.FingR-GFP does indeed label functional inhibitory synapses.

PSD95.FingR and GPHN.FingR label their endogenous target proteins in dissociated neurons, as well as in neurons in slices. To determine whether FingRs can be used to label endogenous proteins in vivo, we transfected PSD95.FingR-GFP into neurons in mouse embryos in utero using electroporation and then assessed expression at approximately 7 weeks of age. Images of dendrites of layer V cortical pyramidal neurons coexpressing HA-mCherry and taken from unstained sections cut from perfused, fixed brains clearly show punctate patterns of GFP expression consistent with labeling of PSD-95 (Figures 9A and 9B). In addition, lower-magnification images show labeling of layer V and layer II/III pyramidal neurons that is also consistent PSD-95 labeling (Figures 9C and 9D). Finally, an image obtained from a living animal of PSD95.FingR-GFP expressed in an apical tuft from a cortical pyramidal neuron (Figure 9E) demonstrates that PSD95.FingR-GFP can be imaged in vivo.

DISCUSSION

In this paper we demonstrate that Fibronectin intrabodies generated with mRNA display (FingRs) can be used to visualize

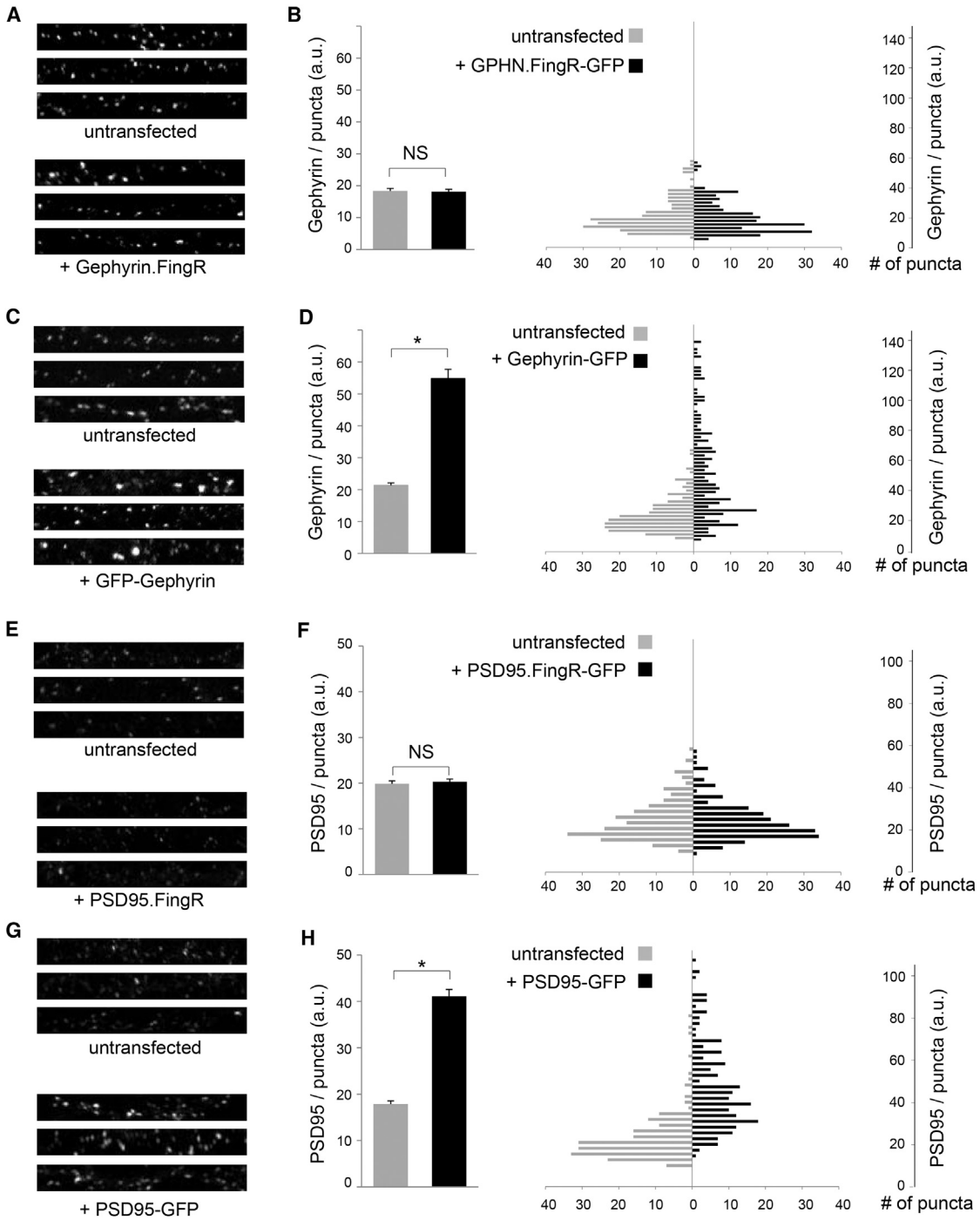

Figure 6. Expression of FingRs Does Not Change the Size of Gephyrin or PSD-95 Puncta

(A) Immunostained Gephyrin puncta from untransfected cells and cells transfected with GPHN.FingR-GFP are of similar size and brightness.

(B) The average intensity associated with Gephyrin puncta is not significantly different in neurons expressing GPHN.FingR-GFP versus untransfected neurons ($p > 0.5$). The amounts of Gephyrin/puncta are distributed similarly in neurons expressing GPHN.FingR-GFP versus untransfected neurons.

(C) Puncta stained with an anti-Gephyrin antibody from cells transfected with Gephyrin-GFP tend to be brighter and larger than those from untransfected cells.

(D) The average intensity associated with Gephyrin puncta is significantly larger in neurons expressing Gephyrin-GFP versus untransfected neurons ($p < 0.0001$). In cells expressing Gephyrin-GFP the amount of Gephyrin/puncta is distributed over a larger range encompassing higher values as compared with similar measurements in untransfected cells. Note that vertical axes of the histograms in (B) and (D) have the same scale.

(E) Puncta stained with an anti-PSD-95 antibody from untransfected cells and cells transfected with PSD95.FingR-GFP are of similar size and brightness.

(F) The average intensity associated with PSD-95 puncta is not significantly different in neurons expressing PSD95.FingR-GFP versus untransfected neurons ($p > 0.5$). The amounts of PSD-95/puncta are distributed similarly in neurons expressing PSD95.FingR-GFP versus untransfected neurons.

(legend continued on next page)

the localization of the endogenous postsynaptic proteins Gephyrin and PSD-95 in living neurons without affecting neuronal structure and function. FingRs represent a substantial improvement over traditional antibody approaches that, in general, require that cells be fixed and permeabilized prior to staining. In addition, FingRs are genetically encoded so that they can be expressed in neurons using methods of transfection and transgenesis that can produce cell-specific expression patterns that are easily interpretable. Expressing FingRs is superior to expressing tagged, exogenous neuronal proteins that tend not to localize in the same manner as their endogenous counterparts and that can cause morphological and functional phenotypes (El-Husseini et al., 2000). Finally, FingR expression is controlled by a transcriptional feedback system, based on a zinc-finger DNA binding domain that closely matches the amount of FingR expressed to that of its endogenous target. Thus, transcriptional regulation allows FingRs to accurately report not just the localization of a protein, but also its expression level.

The innovations in methodology that we have devised here could also be useful for generating FingRs against proteins other than PSD-95 and Gephyrin. We used as targets multimerization domains of cytoskeletal proteins because they provide a rigid surface that FingRs can bind to without disrupting protein function. We screened FingRs produced by mRNA display using an intracellular assay to identify binders that work efficiently in the cytoplasm. Finally, we regulated the FingR transcription using a zinc finger-based negative feedback system. When using this system to produce novel FingRs it should be noted that, as with antibodies, the utility of each FingR is limited by its specific characteristics. Each new FingR must be optimized to bind its target specifically and with high affinity over long periods of time. In addition, each FingR must be thoroughly tested to determine whether binding to its target disrupts the target's functional properties or the ability of the target to interact with other molecules. Regulation must also be tested to ensure that FingR expression can respond dynamically to changes in target. Finally, these properties need to be assessed in the contexts in which the FingRs will be applied.

The properties of PSD-95 and Gephyrin suggest that the FingRs discussed in this paper will be useful for many applications. PSD-95 as well as its homologs PSD-93, SAP-102, and SAP-97 interact either directly or indirectly with AMPA receptors (Dakoji et al., 2003; Leonard et al., 1998) and have been shown to be markers for the size and location of postsynaptic densities (Brenman et al., 1996; Cho et al., 1992; Müller et al., 1996; Valtschanoff et al., 2000). Although dendritic spines have been used as morphological markers of excitatory postsynaptic sites, there is only a rough correlation between synapse size and spine size (Harris and Stevens, 1989). With PSD95.FingR it will now be possible to precisely map the sizes and locations of excitatory postsynaptic sites. The potential applications of GPHN.FingR are even greater, as there is no morphological structure comparable to a dendritic spine that marks inhibitory synapses. For instance, we showed that GPHN.FingR-GFP could be used to identify sites where GABA can be uncaged near inhibitory synapses, enabling a paradigm for probing inhibitory circuitry. In addition, the amount of Gephyrin at postsynaptic inhibitory sites is precisely correlated with the number of GABA or Glycine receptors (Essrich et al., 1998) and thus with the strength of the corresponding inhibitory synaptic connection. Gephyrin and PSD-95 FingRs, therefore, provide a map of the location and strengths of synaptic connections onto specific neurons. We have expressed FingRs in cultured neurons, in slices, and in intact mice using in utero electroporation, suggesting that FingRs will be useful for mapping synaptic connections in many different contexts. Note that because PSD95.FingR-GFP labels the MAGUK proteins SAP-102 and SAP-97 in cultured cells, caution must be used when interpreting its expression pattern in tissue where MAGUK proteins other than PSD-95 are present. However, an advantage of this nonspecific labeling is that PSD95.FingR-GFP can be used to mark synapses in neurons in which PSD-95 is either absent or present at a low level.

One possible application of PSD95.FingR and GPHN.FingR is in the study of how neurons respond to changes in firing rate by tuning the strengths of synaptic inputs (Watt et al., 2000). Previously it has not been possible to monitor strengths of individual excitatory or inhibitory synapses during this tuning process. With the FingRs described in this paper it will now be possible to measure synaptic strengths, providing temporal and spatial information about homeostatic responses in individual neurons. FingRs could also be used in other paradigms where synaptic strength changes are induced, such as LTP and LTD. These experiments could probe how synaptic inputs are controlled with a temporal and/or spatial precision that surpasses current methods. Finally, PSD95.FingR and GPHN.FingR could be used to monitor the changes in synaptic strength in the brains of living mice that occur during behavioral paradigms, for instance during sleep and wake cycles or before and after learning a cognitive task. Thus, with the FingRs generated in this study it may be possible to correlate changes in synaptic structure with events at the cell, circuit, and behavioral levels.

EXPERIMENTAL PROCEDURES

Target Preparation, mRNA Display, and Intracellular Screening

Targets for the mRNA screens consisted of the G domain of Gephyrin ($GPHN_{[1-113]}$) or the SH3-GK domains of PSD-95 ($PSD\text{-}95_{[417-724]}$) fused to a biotin acceptor tag (AviTag, Avidity). mRNA display was carried out essentially as described (Olson et al., 2008). For screening for FingRs that were well-behaved in vivo, GFP-tagged candidates were coexpressed in COS cells with fusion proteins consisting of their respective target (Gephyrin or PSD-95) fused to a Golgi localization signal from the G1 protein of Uukuniemi virus (Andersson et al., 1997). After 14 hr of expression cells were fixed and

(G) Puncta stained with an anti-PSD-95 antibody from cells transfected with PSD95-GFP tend to be brighter and larger than those from untransfected cells. (H) The average intensity associated with PSD-95 puncta is significantly larger in neurons expressing PSD95-GFP versus untransfected neurons ($p < 0.0001$). In cells expressing PSD95-GFP the amount of PSD-95/puncta is distributed over a larger range encompassing higher values as compared with similar measurements in untransfected cells. Note that vertical axes of the histograms in (F) and (H) have the same scale.
All error bars represent SEM. See also Figure S4.

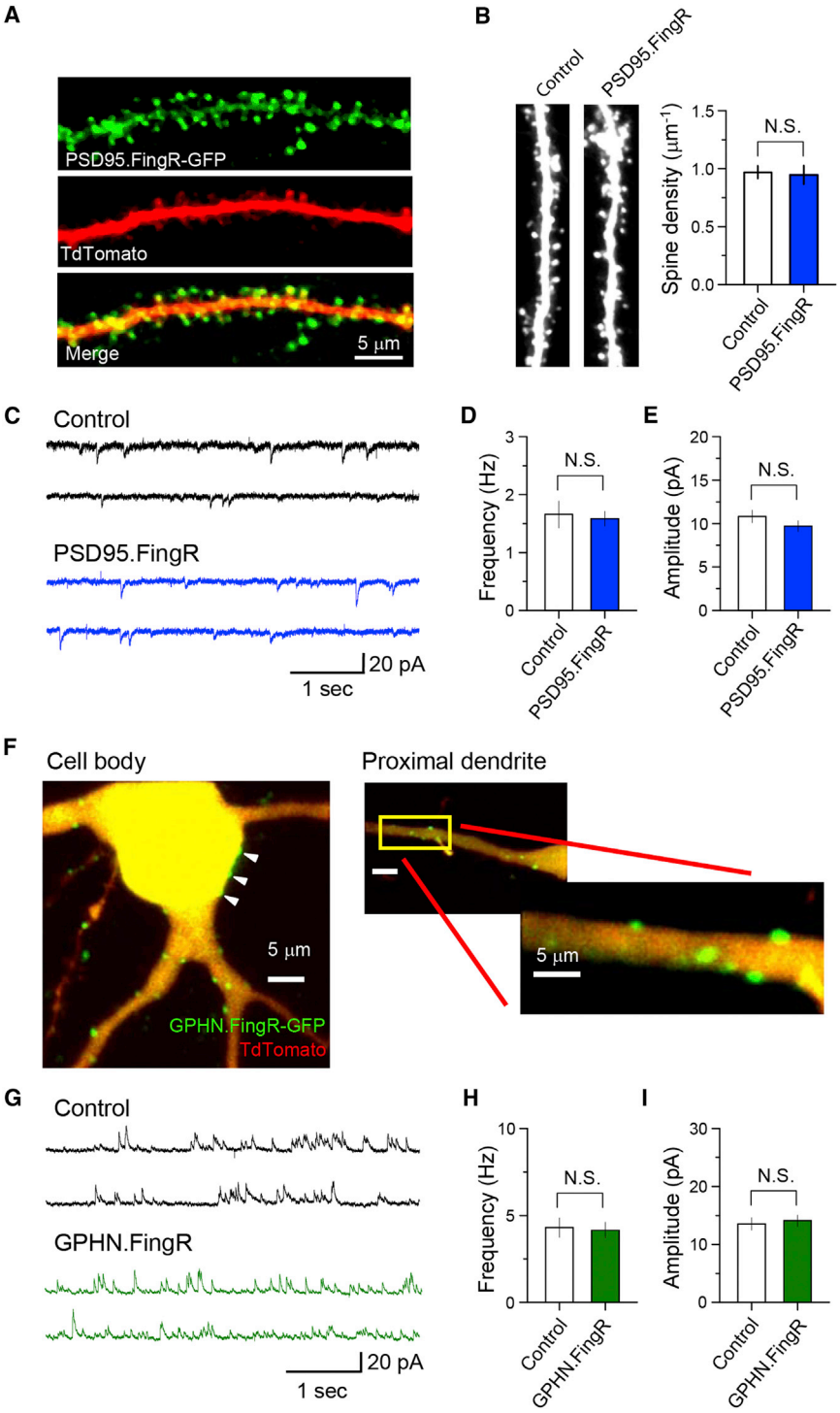

Figure 7. The Presence of FingRs Does Not Change the Morphology or Electrophysiological Properties of Neurons in Hippocampal Slices

(A) PSD95.FingR-GFP (green) expressed in CA1 neurons of the hippocampus shows punctate staining of spine heads, consistent with staining at postsynaptic sites, which is distinct from the pattern of coexpressed TdTomato (red).

(B) The morphology of dendrites in cells expressing PSD95.FingR-GFP was not qualitatively different from control cells. Similarly, spine density was not significantly different between cells expressing PSD95.FingR-GFP and control cells.

(C–E) mEPSCs from cells expressing PSD95.FingR-GFP (C) were not qualitatively different from those recorded from control cells. In addition, the frequencies (D) and amplitudes (E) of mEPSCs did not differ between cells expressing PSD95.FingR-GFP and control cells.

(F) In a cell expressing GPHN.FingR-GFP (green) and TdTomato (red), the FingR expresses in puncta on the dendritic shaft in a manner similar to inhibitory postsynaptic sites.

(G) mIPSCs recorded from cells expressing GPHN.FingR-GFP do not differ qualitatively from mIPSCs from untransfected control neurons (H).

(I) Similarly, neither the frequency nor the amplitude of mIPSCs recorded from cells expressing GPHN.FingR-GFP differed significantly from those recorded from control cells.

All error bars represent SEM.

stained, and FingRs were selected on the basis of colocalization with Golgi-restricted target.

Immunocytochemistry, Imaging, and Data Analysis

Immunocytochemistry of dissociated cultures was performed as in (Lewis et al., 2009). Fixed dissociated cortical neurons were imaged on an Olympus FV1000 confocal microscope. Pixel intensity levels were measured with ImageJ (U.S. National Institutes of Health). All analyses were performed blinded. Live cells were imaged on an Olympus IX81 microscope. All analysis was performed by blinded observers.

In Utero Electroporation and In Vivo Imaging

Electroporations were performed as described in (Saito, 2006). Cranial windows were inserted as described in (Holtmaat et al., 2005). Live images

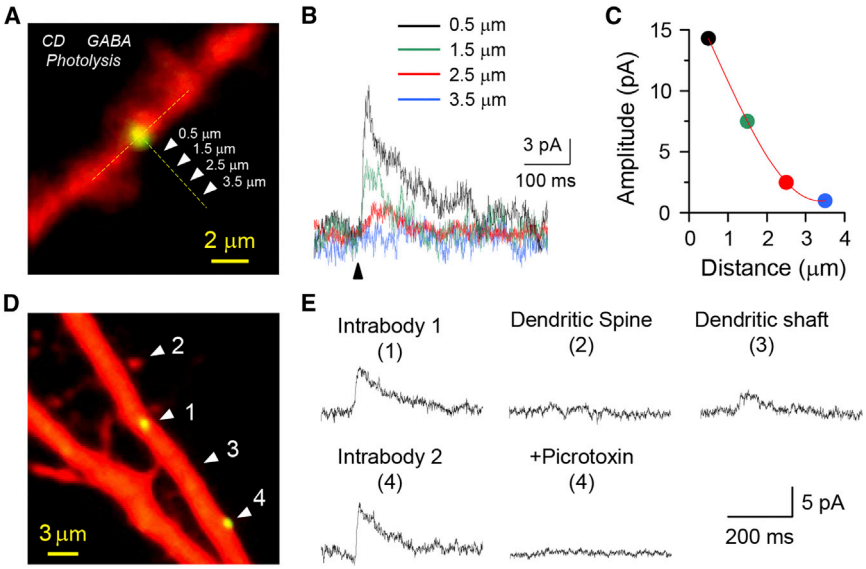

Figure 8. Puncta of GPHN.FingR-GFP Intrabody Recognized by GFP Fluorescence Represent Clusters of Ionotropic GABA Receptors

(A–C) Apical dendrite of CA1 pyramidal neurons (A) in an oganotypic slice culture showing the locations of serial GABA uncaging by two-photon-mediated photorelease from CDNI-GABA. (B and C) Resulting inward currents reveal a rapid fall off in the amplitude of IPSCs with distance from the GFP punctum.

(D) Lower-magnification image of additional dendrite with several labeled GFP puncta and dendritic spines.

(E) Representative traces during GABA photorelease at two locations (2, 3) that were not near GPHN.FingR-GFP puncta (one on a dendritic spine and a second on the shaft) and at two locations (1, 4) next to GPHN.FingR-GFP puncta located on the dendritic shaft. The currents are blocked by picrotoxin, as expected for ionotropic GABA receptors.

were acquired with a Movable Objective Microscope (MOM) (Sutter Instruments). Experimental protocols were conducted according to the U.S. National Institutes of Health guidelines for animal research and were approved by the Institutional Animal Care and Use Committee at the University of Southern California.

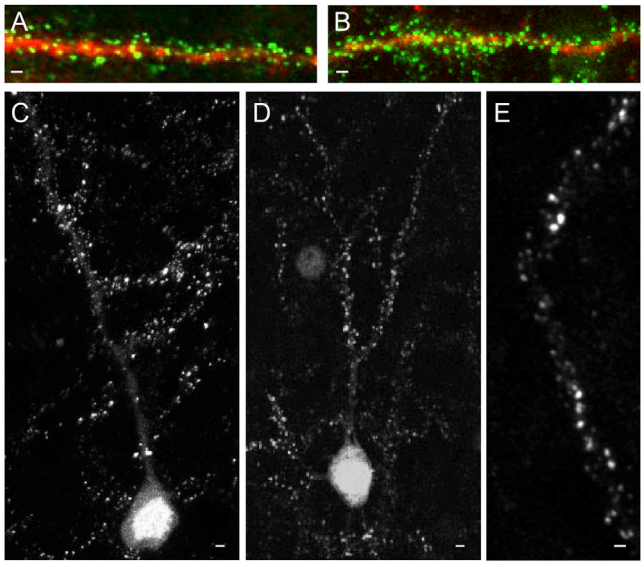

Figure 9. Expression of PSD95.FingR-GFP In Vivo

(A and B) Apical dendrites from a layer V cortical pyramidal neuron expressing PSD95.FingR-GFP (green) and HAmCherry (red). Cells were present in fixed sections cut from 7-week-old mice that were electroporated in utero.

(C) Layer V cortical pyramidal neuron expressing PSD95.FingR-GFP from section prepared in the same manner as in (A) and (B).

(D) Layer II/III cortical neuron expressing PSD95.FingR-GFP from section prepared in the same manner as in (A) and (B).

(E) Live two-photon image of a tuft of an apical dendrite from a cortical pyramidal neuron. Image was taken through a cranial window in a 7-week-old mouse expressing PSD95.FingR-GFP. Scale bar represents 5 µm.

SUPPLEMENTAL INFORMATION

Supplemental Information includes Supplemental Experimental Procedures, four figures, and one movie and can be found with this article online at http://dx.doi.org/10.1016/j.neuron.2013.04.017.

ACKNOWLEDGMENTS

We thank Liana Asatryan (USC, Lentivirus Core Facility) for producing lentivirus, Aaron Nichols for help in producing the naive FingR library, Samantha Ancona-Esselmann for technical assistance and help in data analysis, Jerardo Viramontes Garcia for help in data analysis, and Ryan Kast for technical help with in vivo two-photon imaging. We thank Matthew Pratt, David McKemy, Samantha Butler, and members of the Arnold and Roberts laboratories for helpful suggestions on the manuscript. D.B.A. was supported by grants GM-083898 and MH-086381. R.W.R. was supported by GM-083898, GM 060416, and OD 006117. G.C.R.E.-D. was supported by GM53395 and NS69720. B.L.S. was supported by NS-046579. G.C.R.E.-D. has filed a preliminary patent declaration on the synthesis of dinitroindolinyl-caged neurotransmitters.

Accepted: April 10, 2013
Published: June 19, 2013

REFERENCES

Andersson, A.M., Melin, L., Bean, A., and Pettersson, R.F. (1997). A retention signal necessary and sufficient for Golgi localization maps to the cytoplasmic tail of a Bunyaviridae (Uukuniemi virus) membrane glycoprotein. J. Virol. *71*, 4717–4727.

Arnold, D.B., and Clapham, D.E. (1999). Molecular determinants for subcellular localization of PSD-95 with an interacting K+ channel. Neuron *23*, 149–157.

Brenman, J.E., Christopherson, K.S., Craven, S.E., McGee, A.W., and Bredt, D.S. (1996). Cloning and characterization of postsynaptic density 93, a nitric oxide synthase interacting protein. J. Neurosci. *16*, 7407–7415.

Brenman, J.E., Topinka, J.R., Cooper, E.C., McGee, A.W., Rosen, J., Milroy, T., Ralston, H.J., and Bredt, D.S. (1998). Localization of postsynaptic density-93 to dendritic microtubules and interaction with microtubule-associated protein 1A. J. Neurosci. *18*, 8805–8813.

Burkhalter, A., Gonchar, Y., Mellor, R.L., and Nerbonne, J.M. (2006). Differential expression of I(A) channel subunits Kv4.2 and Kv4.3 in mouse visual cortical neurons and synapses. J. Neurosci. *26*, 12274–12282.

Chalfie, M., Tu, Y., Euskirchen, G., Ward, W.W., and Prasher, D.C. (1994). Green fluorescent protein as a marker for gene expression. Science *263*, 802–805.

Chiu, C.S., Jensen, K., Sokolova, I., Wang, D., Li, M., Deshpande, P., Davidson, N., Mody, I., Quick, M.W., Quake, S.R., and Lester, H.A. (2002). Number, density, and surface/cytoplasmic distribution of GABA transporters at presynaptic structures of knock-in mice carrying GABA transporter subtype 1-green fluorescent protein fusions. J. Neurosci. *22*, 10251–10266.

Cho, K.O., Hunt, C.A., and Kennedy, M.B. (1992). The rat brain postsynaptic density fraction contains a homolog of the Drosophila discs-large tumor suppressor protein. Neuron *9*, 929–942.

Chu, P.J., Rivera, J.F., and Arnold, D.B. (2006). A role for Kif17 in transport of Kv4.2. J. Biol. Chem. *281*, 365–373.

Coons, A.H., Creech, H.J., Jones, R.N., and Berliner, E. (1942). Demonstration of pneumoccocal antigen in tissues by use of fluorescent antibody. J. Immunol. *45*, 159–170.

Craig, A.M., Banker, G., Chang, W., McGrath, M.E., and Serpinskaya, A.S. (1996). Clustering of gephyrin at GABAergic but not glutamatergic synapses in cultured rat hippocampal neurons. J. Neurosci. *16*, 3166–3177.

Dakoji, S., Tomita, S., Karimzadegan, S., Nicoll, R.A., and Bredt, D.S. (2003). Interaction of transmembrane AMPA receptor regulatory proteins with multiple membrane associated guanylate kinases. Neuropharmacology *45*, 849–856.

Dickinson, C.D., Veerapandian, B., Dai, X.-P., Hamlin, R.C., Xuong, N.H., Ruoslahti, E., and Ely, K.R. (1994). Crystal structure of the tenth type III cell adhesion module of human fibronectin. J. Mol. Biol. *236*, 1079–1092.

El-Husseini, A.E., Schnell, E., Chetkovich, D.M., Nicoll, R.A., and Bredt, D.S. (2000). PSD-95 involvement in maturation of excitatory synapses. Science *290*, 1364–1368.

Essrich, C., Lorez, M., Benson, J.A., Fritschy, J.M., and Lüscher, B. (1998). Postsynaptic clustering of major GABAA receptor subtypes requires the gamma 2 subunit and gephyrin. Nat. Neurosci. *1*, 563–571.

Gabriel, R., Lombardo, A., Arens, A., Miller, J.C., Genovese, P., Kaeppel, C., Nowrouzi, A., Bartholomae, C.C., Wang, J., Friedman, G., et al. (2011). An unbiased genome-wide analysis of zinc-finger nuclease specificity. Nat. Biotechnol. *29*, 816–823.

Goto, Y., and Hamaguchi, K. (1979). The role of the intrachain disulfide bond in the conformation and stability of the constant fragment of the immunoglobulin light chain. J. Biochem. *86*, 1433–1441.

Goto, Y., Tsunenaga, M., Kawata, Y., and Hamaguchi, K. (1987). Conformation of the constant fragment of the immunoglobulin light chain: effect of cleavage of the polypeptide chain and the disulfide bond. J. Biochem. *101*, 319–329.

Harris, K.M., and Stevens, J.K. (1989). Dendritic spines of CA 1 pyramidal cells in the rat hippocampus: serial electron microscopy with reference to their biophysical characteristics. J. Neurosci. *9*, 2982–2997.

Holtmaat, A.J., Trachtenberg, J.T., Wilbrecht, L., Shepherd, G.M., Zhang, X., Knott, G.W., and Svoboda, K. (2005). Transient and persistent dendritic spines in the neocortex in vivo. Neuron *45*, 279–291.

Huston, J.S., Levinson, D., Mudgett-Hunter, M., Tai, M.-S., Novotný, J., Margolies, M.N., Ridge, R.J., Bruccoleri, R.E., Haber, E., Crea, R., et al. (1988). Protein engineering of antibody binding sites: recovery of specific activity in an anti-digoxin single-chain Fv analogue produced in Escherichia coli. Proc. Natl. Acad. Sci. USA *85*, 5879–5883.

Ishikawa, F.N., Chang, H.-K., Curreli, M., Liao, H.I., Olson, C.A., Chen, P.C., Zhang, R., Roberts, R.W., Sun, R., Cote, R.J., et al. (2009). Label-free, electrical detection of the SARS virus N-protein with nanowire biosensors utilizing antibody mimics as capture probes. ACS Nano *3*, 1219–1224.

Jinno, S., Jeromin, A., and Kosaka, T. (2005). Postsynaptic and extrasynaptic localization of Kv4.2 channels in the mouse hippocampal region, with special reference to targeted clustering at gabaergic synapses. Neuroscience *134*, 483–494.

Kanaani, J., el-Husseini, Ael.-D., Aguilera-Moreno, A., Diacovo, J.M., Bredt, D.S., and Baekkeskov, S. (2002). A combination of three distinct trafficking signals mediates axonal targeting and presynaptic clustering of GAD65. J. Cell Biol. *158*, 1229–1238.

Karatan, E., Merguerian, M., Han, Z., Scholle, M.D., Koide, S., and Kay, B.K. (2004). Molecular recognition properties of FN3 monobodies that bind the Src SH3 domain. Chem. Biol. *11*, 835–844.

Koide, A., Bailey, C.W., Huang, X., and Koide, S. (1998). The fibronectin type III domain as a scaffold for novel binding proteins. J. Mol. Biol. *284*, 1141–1151.

Langosch, D., Hoch, W., and Betz, H. (1992). The 93 kDa protein gephyrin and tubulin associated with the inhibitory glycine receptor are phosphorylated by an endogenous protein kinase. FEBS Lett. *298*, 113–117.

Leonard, A.S., Davare, M.A., Horne, M.C., Garner, C.C., and Hell, J.W. (1998). SAP97 is associated with the alpha-amino-3-hydroxy-5-methylisoxazole-4-propionic acid receptor GluR1 subunit. J. Biol. Chem. *273*, 19518–19524.

Lewis, T.L., Jr., Mao, T., Svoboda, K., and Arnold, D.B. (2009). Myosin-dependent targeting of transmembrane proteins to neuronal dendrites. Nat. Neurosci. *12*, 568–576.

Lu, W., Isozaki, K., Roche, K.W., and Nicoll, R.A. (2010). Synaptic targeting of AMPA receptors is regulated by a CaMKII site in the first intracellular loop of GluA1. Proc. Natl. Acad. Sci. USA *107*, 22266–22271.

Main, A.L., Harvey, T.S., Baron, M., Boyd, J., and Campbell, I.D. (1992). The three-dimensional structure of the tenth type III module of fibronectin: an insight into RGD-mediated interactions. Cell *71*, 671–678.

Mani, M., Kandavelou, K., Dy, F.J., Durai, S., and Chandrasegaran, S. (2005). Design, engineering, and characterization of zinc finger nucleases. Biochem. Biophys. Res. Commun. *335*, 447–457.

Margolin, J.F., Friedman, J.R., Meyer, W.K., Vissing, H., Thiesen, H.J., and Rauscher, F.J., 3rd. (1994). Krüppel-associated boxes are potent transcriptional repression domains. Proc. Natl. Acad. Sci. USA *91*, 4509–4513.

Marshall, J., Molloy, R., Moss, G.W., Howe, J.R., and Hughes, T.E. (1995). The jellyfish green fluorescent protein: a new tool for studying ion channel expression and function. Neuron *14*, 211–215.

McGee, A.W., Dakoji, S.R., Olsen, O., Bredt, D.S., Lim, W.A., and Prehoda, K.E. (2001). Structure of the SH3-guanylate kinase module from PSD-95 suggests a mechanism for regulated assembly of MAGUK scaffolding proteins. Mol. Cell *8*, 1291–1301.

Müller, B.M., Kistner, U., Kindler, S., Chung, W.J., Kuhlendahl, S., Fenster, S.D., Lau, L.F., Veh, R.W., Huganir, R.L., Gundelfinger, E.D., and Garner, C.C. (1996). SAP102, a novel postsynaptic protein that interacts with NMDA receptor complexes in vivo. Neuron *17*, 255–265.

Naisbitt, S., Kim, E., Tu, J.C., Xiao, B., Sala, C., Valtschanoff, J., Weinberg, R.J., Worley, P.F., and Sheng, M. (1999). Shank, a novel family of postsynaptic density proteins that binds to the NMDA receptor/PSD-95/GKAP complex and cortactin. Neuron *23*, 569–582.

Nizak, C., Monier, S., del Nery, E., Moutel, S., Goud, B., and Perez, F. (2003). Recombinant antibodies to the small GTPase Rab6 as conformation sensors. Science *300*, 984–987.

Olson, C.A., and Roberts, R.W. (2007). Design, expression, and stability of a diverse protein library based on the human fibronectin type III domain. Protein Sci. *16*, 476–484.

Olson, C.A., Liao, H.-I., Sun, R., and Roberts, R.W. (2008). mRNA display selection of a high-affinity, modification-specific phospho-IkappaBalpha-binding fibronectin. ACS Chem. Biol. *3*, 480–485.

Prior, P., Schmitt, B., Grenningloh, G., Pribilla, I., Multhaup, G., Beyreuther, K., Maulet, Y., Werner, P., Langosch, D., Kirsch, J., et al. (1992). Primary structure and alternative splice variants of gephyrin, a putative glycine receptor-tubulin linker protein. Neuron *8*, 1161–1170.

Proba, K., Wörn, A., Honegger, A., and Plückthun, A. (1998). Antibody scFv fragments without disulfide bonds made by molecular evolution. J. Mol. Biol. *275*, 245–253.

Rivera, J.F., Ahmad, S., Quick, M.W., Liman, E.R., and Arnold, D.B. (2003). An evolutionarily conserved dileucine motif in Shal K+ channels mediates dendritic targeting. Nat. Neurosci. *6*, 243–250.

Roberts, R.W., and Szostak, J.W. (1997). RNA-peptide fusions for the *in vitro* selection of peptides and proteins. Proc. Natl. Acad. Sci. USA *94*, 12297–12302.

Saito, T. (2006). In vivo electroporation in the embryonic mouse central nervous system. Nat. Protoc. *1*, 1552–1558.

Shin, S.M., Zhang, N., Hansen, J., Gerges, N.Z., Pak, D.T., Sheng, M., and Lee, S.H. (2012). GKAP orchestrates activity-dependent postsynaptic protein remodeling and homeostatic scaling. Nat. Neurosci. *15*, 1655–1666.

Sola, M., Kneussel, M., Heck, I.S., Betz, H., and Weissenhorn, W. (2001). X-ray crystal structure of the trimeric N-terminal domain of gephyrin. J. Biol. Chem. *276*, 25294–25301.

Southwell, A.L., Khoshnan, A., Dunn, D.E., Bugg, C.W., Lo, D.C., and Patterson, P.H. (2008). Intrabodies binding the proline-rich domains of mutant huntingtin increase its turnover and reduce neurotoxicity. J. Neurosci. *28*, 9013–9020.

Takagi, T., Pribilla, I., Kirsch, J., and Betz, H. (1992). Coexpression of the receptor-associated protein gephyrin changes the ligand binding affinities of alpha 2 glycine receptors. FEBS Lett. *303*, 178–180.

Tu, J.C., Xiao, B., Naisbitt, S., Yuan, J.P., Petralia, R.S., Brakeman, P., Doan, A., Aakalu, V.K., Lanahan, A.A., Sheng, M., and Worley, P.F. (1999). Coupling of mGluR/Homer and PSD-95 complexes by the Shank family of postsynaptic density proteins. Neuron *23*, 583–592.

Valtschanoff, J.G., Burette, A., Davare, M.A., Leonard, A.S., Hell, J.W., and Weinberg, R.J. (2000). SAP97 concentrates at the postsynaptic density in cerebral cortex. Eur. J. Neurosci. *12*, 3605–3614.

Varley, Z.K., Pizzarelli, R., Antonelli, R., Stancheva, S.H., Kneussel, M., Cherubini, E., and Zacchi, P. (2011). Gephyrin regulates GABAergic and glutamatergic synaptic transmission in hippocampal cell cultures. J. Biol. Chem. *286*, 20942–20951.

Watt, A.J., van Rossum, M.C., MacLeod, K.M., Nelson, S.B., and Turrigiano, G.G. (2000). Activity coregulates quantal AMPA and NMDA currents at neocortical synapses. Neuron *26*, 659–670.

Witzgall, R., O'Leary, E., Leaf, A., Onaldi, D., and Bonventre, J.V. (1994). The Krüppel-associated box-A (KRAB-A) domain of zinc finger proteins mediates transcriptional repression. Proc. Natl. Acad. Sci. USA *91*, 4514–4518.

Xu, L., Aha, P., Gu, K., Kuimelis, R.G., Kurz, M., Lam, T., Lim, A.C., Liu, H., Lohse, P.A., Sun, L., et al. (2002). Directed evolution of high-affinity antibody mimics using mRNA display. Chem. Biol. *9*, 933–942.

Yu, W., Jiang, M., Miralles, C.P., Li, R.W., Chen, G., and de Blas, A.L. (2007). Gephyrin clustering is required for the stability of GABAergic synapses. Mol. Cell. Neurosci. *36*, 484–500.